LETTER

# Qubit(s) transfer in helical spin chains

A Letters Journal Exploring the Frontiers of Physics

August 2017

EPL, **119** (2017) 30001 www.epljournal.org
doi: 10.1209/0295-5075/119/30001

# Qubit(s) transfer in helical spin chains

Harshit Verma[1], L. Chotorlishvili[2], J. Berakdar[2] and Sunil K. Mishra[1]

[1] *Department of Physics, Indian Institute of Technology (Banaras Hindu University) - Varanasi, 221005, India*
[2] *Institut für Physik, Martin-Luther-Universität Halle-Wittenberg - D-06099 Halle, Germany*

received 31 July 2017; accepted in final form 12 September 2017
published online 16 October 2017

PACS 03.67.Hk – Quantum communication
PACS 75.85.+t – Magnetoelectric effects, multiferroics
PACS 75.10.Pq – Spin chain models

**Abstract** – Qubit(s) transfer through a helical chain is studied. We consider the transfer of a single state and Bell states across a multiferroic spin chain and the possibility of an electric-field control of the fidelity of the single state and the Bell pairs. We analyze pure and imperfect multiferroic spin chains. A scheme for an efficient transfer of spin states through a multiferroic channel relies on kicking by appropriate electric-field pulses at regular intervals. This electric-field pulse sequence undermines the effect of impurity on the fidelity and improves the state transfer through the helical chain.



**Introduction.** – Spin chains have long been studied as a credible contender for carrying out quantum information processing and transmission [1–12]. Various new experiments have been carried out and numerous models proposed for spin chain systems [13–15]. The systems of interest in the present paper is a multiferroic spin chain through which, we seek to transfer quantum information or qubits. Multiferroic systems possess intrinsically coupled magnetic and ferroelectric order parameters [16–19]. Hence, the strong magnetoelectric coupling can be utilized as a tool in quantum information processing. For spin-driven emergence of ferroelectric polarization, the ferroelectric order parameter is directly related to the non-collinear magnetic order. The ferroelectric polarization vanishes in the collinear magnetic (ferro or antiferromagnetic) phase, while in case of a chiral spin order a net polarization remains that can couple to an external electric field thus allowing for an electric-field control of the magnetic order. Under a certain geometry of the system and the applied external fields, the magnetoelectric coupling term mimics the dynamical Dzyaloshinskii-Moriya interaction. Breaking of the inversion symmetry associated with the Dzyaloshinskii-Moriya interaction may have key consequences for the transfer of quantum information. We first investigate the transmission of qubits through a multiferrroic chain with a static constant electric field and then also introduce the electric-field kicks at a regular interval. It is noteworthy that a continuous application of the electric field with changing the amplitude leads to a complex nature of the time evolution operator, *i.e.* of an integral form due to the non-commutation of the exchange interaction and the Dzyaloshinskii-Moriya interaction terms in the Hamiltonian.

Realistic systems always have a defect (pinning centers) and/or embedded impurities. Therefore, the study of the pinning centers and the embedded impurities is not only of an academic but also of a practical interest. To be more realistic we consider the effect of doping the spin chain, *i.e.* introducing impurities at specific sites and constructing various new models considering the types of impurity. Embedded impurities locally modify the strength of the exchange interaction and break the translational invariance. A naive guess is that the impurity or the pining center embedded in the system hinders the propagation of the excitation through the chain. We find, as far as the quantum state transfer fidelity is concerned, the picture is not trivial. Studying the possibility of the transmission of a single qubit through the impurity-embedded spin chain with realistic material parameters we identify case of a better transmission of the qubit (or at least on par) as compared to a pure spin chain. Some particular recipes for an effective transfer of qubits are analyzed.

Initially, the system is prepared in fully polarized state (all spins down). The qubit is injected to the first site of the spin chain and received at the last site. The parameter for good transmission named "fidelity" is discussed later and the expression is calculated elsewhere given these initial conditions and information injection approach. Such a transmission has practical applications insofar as various quantum communication protocols require the sender and

the receiver to share one qubit each of a Bell pair [20]. We also explore the possibility of transfer of Bell pair directly by injecting it to the first two qubits of the spin chain and subsequently receiving them at the last and second last sites of the chain. The transmission channel in our case, of course, is an open chain.

The paper is organized as follows: Firstly, we specify the model and its Hamiltonian. Next, we provide analytical expressions of the quantum state transfer fidelity for a single qubit and for Bell states. Lastly, we discuss the results of numerical calculations before summarizing the study.

**Models.** – The Hamiltonian of the multiferroic system reads [12]

$$\mathcal{H} = -J_1 \sum_i \vec{S}_i.\vec{S}_{i+1} - J_2 \sum_i \vec{S}_i.\vec{S}_{i+2} + B\sum_i \vec{S}_i^z + \mathcal{E}(t) g_{ME} \sum_i \left(\vec{S}_i \times \vec{S}_{i+1}\right)^z. \quad (1)$$

The constants $J_1$ and $J_2$ characterize the nearest and next-nearest-neighbour interaction strengths. Taking competing nearest ferromagnetic $J_1 > 0$ and next-nearest ferromagnetic $J_2 < 0$ antiferromagnetic interactions lead to a spin frustration and a non-collinear spin order. $B$ is the magnetic field and $\mathcal{E}(t)$ is the electric field coupled to the ferroelectric polarization. $g_{ME}$ is the magnetoelectric coupling strength. The time varying electric field affects the electric polarization $\vec{P}$ in a manner such that $-\vec{\mathcal{E}}(t)\cdot\vec{P} = \mathcal{E}(t) g_{ME} \sum_i \left(\vec{S}_i \times \vec{S}_{i+1}\right)^z$. Here $\left(\vec{S}_i \times \vec{S}_{i+1}\right)^z$ is the $z$-component of the vector chirality. The time-dependent electric field $E(t) = g_{ME}\mathcal{E}(t)$ has two components, namely the static field $E_0$ at times between the kicks and $E_1$ at $t = n\tau$ *i.e.* at the kick time. The embedded impurity is described by an additional term and the corresponding sites are excluded from the above Hamiltonian according to the subscribed impurity model. We adopt open boundary conditions in all the cases discussed in the paper. We consider the following cases in the paper.

*Pure spin chain with kicked electric field.* The Hamiltonian considered is the above one but with a peculiar twist: Apart from a small static electric field which is switched on at all times, the system is also kicked with an electric-field pulse at regular time intervals. The temporal profile of the kicking electric field can be taken as delta function, meaning that the actual duration of the electric-field pulse is much smaller that the characteristic time scale of the system (in our case below this time scale is in the ps regime, in which case sub-ps electric (laser) field pulses are suitable) [21]. As discussed in [21] such pulses allow a non-perturbative treatment of the non-equilibrium quantum dynamics. The kicking scheme is illustrated in fig. 1 and will be used for other spin models in this manuscript. Actually, the Hamiltonian has the

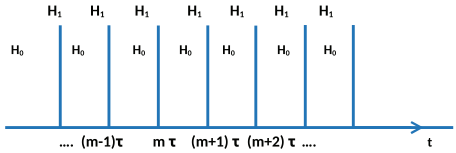


Fig. 1: (Colour online) Kicking scheme showing that the electric field is switched on at a certain regular time interval and can be modelled by delta functions.

following form:

$$\mathcal{H} = \mathcal{H}_0 + \mathcal{H}_1, \quad (2)$$

$$\mathcal{H}_0 = -J_1 \sum_i \vec{S}_i.\vec{S}_{i+1} - J_2 \sum_i \vec{S}_i.\vec{S}_{i+2} + E_0 \sum_i \left(\vec{S}_i \times \vec{S}_{i+1}\right)^z, \quad (3)$$

$$\mathcal{H}_1 = E_1 \sum_{n=1}^{n=\infty} \delta\left(t/\tau - n\right) \sum_i \left(\vec{S}_i \times \vec{S}_{i+1}\right)^z, \quad (4)$$

where $n$ indicates the number of kicks applied, $E_0 = g_{ME}\mathcal{E}_0$ the static background field and $E_1 = g_{ME}\mathcal{E}_1$ the amplitude of the kicked field. Only at the interval of $\tau$ does the electric field kick term assume non-zero value and contributes to the Hamiltonian. We have confined our studies to the effect of electric field only and hence $B_z = 0$ at all times. The time evolution operator evaluated between $m\tau_+$ and $(m+1)\tau_+$ (here $t_+$ denotes the time just after the kick) is given by $U(m) = (\hat{\mathcal{U}}_1\,\hat{\mathcal{U}}_0)^m$ [22], where

$$\hat{\mathcal{U}}_0 = \exp\left(iJ_1\tau \sum_i \vec{S}_i.\vec{S}_{i+1} + iJ_2\tau \sum_i \vec{S}_i.\vec{S}_{i+2} - iE_0 \sum_i \left(\vec{S}_i \times \vec{S}_{i+1}\right)^z\right),$$

$$\hat{\mathcal{U}}_1 = \exp\left(-iE_1 \sum_i \left(\vec{S}_i \times \vec{S}_{i+1}\right)^z\right), \quad (5)$$

and the state after the $m$-th kick (or at time $t = m\tau_+$) is

$$|\psi(t = m\tau_+)\rangle = \left(\hat{\mathcal{U}}_1\,\hat{\mathcal{U}}_0\right)^m |\psi(t=0)\rangle. \quad (6)$$

*Type-I impurity.* An impurity is introduced at a site (say between $n$ and $n+1$) in the spin chain with the usual nearest-neighbour and the next-nearest-neighbour spin exchange terms. Actually, we consider it to be at the $n+1$ site by modifying the label of the spins. The introduction of an impurity between the $n, n+1$ and $n+1, n+2$ sites may lead to a local modification of the exchange constants $J_1$ and $J_2$ terms for these most affected spins *i.e.* a few surrounding the impurity [23]. Keeping in mind that both nearest and next-nearest exchange interactions remain the same with respect to the impurity, to accommodate this arrangement, the change in the interaction terms between the subsequent neighbours to $n$ and $n+2$ is considered. It is well known and has also been experimentally proved that the lattice spacing does affect the

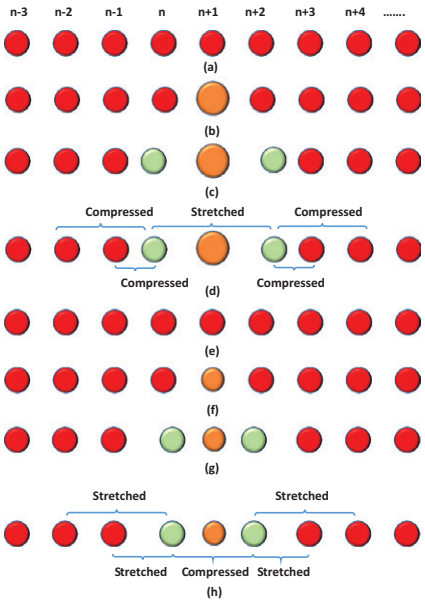


Fig. 2: (Colour online) The introduction of two types of impurities is depicted. Such impurities cause the local compression or elongation of the bonds between its nearest and next-nearest neighbour. In (a) a pure chain is shown. The impurity site is chosen as $n+1$, as shown in (b). In (c) the rearrangement of spins due to type-I impurity is shown. The modification in the nearest-neighbour interaction ($J_1$) and in the next-nearest-neighbour interaction ($J_2$) due to this impurity is shown in (d). The other interactions remain unchanged. Panel (e) again gives a pure spin chain for reference. Impurity site is shown in (f). Panel (g) shows the rearrangement of spins due to the introduction of type-II impurity. The modifications in the nearest-neighbour interaction ($J_1$) and in the next-nearest-neighbour interaction ($J_2$) due to impurity are shown in (h). The other interactions remain unchanged.

exchange integral [24], *i.e.* $J_1$ and $J_2$. We just consider the final effect without going into the microscopic details and the exact relation by which this parameter changes with the lattice spacing. However, the magnitude of increasing/decreasing the distance between the lattice sites due to the embedded impurities is assumed to be in tune with changes in $J_1$ and $J_2$. The following can be noted regarding the impact of introducing such an impurity on the interaction between the sets of two spins surrounding the impurity as shown in fig. 2(a), (b), (c), (d): The nearest-neighbour exchange integrals ($J_1$) are affected: ($n-1$, $n$ —increased ($J_{11}$)), ($n$, $n+1$(impurity) —unchanged), ($n+1$(impurity), $n+2$ —unchanged), ($n+2$, $n+3$ —increased ($J_{11}$)). Next-nearest-neighbour exchange integrals ($J_2$) are affected: ($n-2, n$ —increased ($J_{22}$)), ($n-1, n+1$(impurity) —unchanged), ($n, n+2$ —decreased ($J_{222}$)), ($n+1$(impurity), $n+3$ —unchanged), ($n+2$, $n+4$ —increased ($J_{22}$)). The bonds are being referenced from the zero-impurity model and would correspond to a change in the bond parameters ($J_1$ or $J_2$), *i.e.*, smaller magnitude for the stretched bond and larger magnitude


Fig. 3: (Colour online) Spin channel for transmission of qubit(s). The first two ($s1, s2$) (one) sites are substituted with the Bell pair (single qubit) and correspondingly are received on the other side at sites $r1$, $r2$ (or simply $r2$).

for the compressed bond [24]. In a nutshell, the impurity changes the interaction strength in such a way that the nearest and next-nearest bonds of the impurity are unchanged. Other bonds which are changed are mentioned in fig. 2 and clearly, the effect of introduction of impurity is localized to 3-4 sites near the impurity. The Hamiltonian is modified according to the aforementioned scheme to include the impurity terms.

*Type-II impurity.* The model is the same as the second one but with just one change. The embedded impurity locally reduces the strength of the exchange interaction between nearest and next-nearest-neighbouring spins. Similar to the above, we consider the impurity to be embedded at the $n+1$ site by modifying the label of spins. The following can be noted regarding the impact of interaction between sets of two spins surrounding the impurity as shown in fig. 2 (e), (f), (g), (h):

Nearest-neighbour exchange integrals ($J_1$) are affected: ($n-1$, $n$ —decreased ($J_{111}$)), ($n$, $n+1$(impurity) —unchanged), ($n+1$(impurity), $n+2$ —unchanged), ($n+2$, $n+3$ —decreased ($J_{111}$)). Next-nearest-neighbour exchange integrals ($J_2$) are affected: ($n-2$, $n$ —decreased ($J_{222}$)), ($n-1$, $n+1$(impurity) —unchanged), ($n$, $n+2$ —increased ($J_{22}$)), ($n+1$(impurity), $n+3$ —unchanged), ($n+2$, $n+4$ —decreased ($J_{222}$)). The bond parameters are changed in the same way as discussed in the previous model.

**Fidelity.** – For the purpose of transmission of qubit, fidelity may be used as a figure of merit. Note that as a case in all the models considered, a single spin is substituted at one end of the chain (sender) and the qubit is expected to be transmitted to the other end of the chain (receiver). Also, initially the system is prepared in fully spin down polarized state. The fidelity of qubit transfer is given by [1]: $F = \langle\psi_{in}|\rho_{out}|\psi_{in}\rangle$ which on calculation for a single qubit ($\Omega_0$) comes out to be $F = \frac{|f_{r,s}(t_0)|\cos\gamma}{3} + \frac{|f_{r,s}(t_0)|^2}{6} + \frac{1}{2}$, where $\gamma = \arg(f_{r,s}(t_0))$ and $f_{r,s}(t) = \langle r|\exp(-iHt)|s\rangle$, where $r$ and $s$ are receiver and sender states, respectively, and the Hamiltonian corresponds to a single excitation. A qubit transmitted through a classical channel has a fidelity of 0.66 [1]. Hence, our interest lies in conditions for the above systems to exhibit high fidelity, at least greater than 0.66. Another case in consideration is the transmission of two qubits through the chain with a protocol very similar to the first case, *i.e.*, the qubits are substituted at the sites $s1, s2$ and are received at $r1, r2$ (fig. 3). However, we consider only the case where the maximally entangled

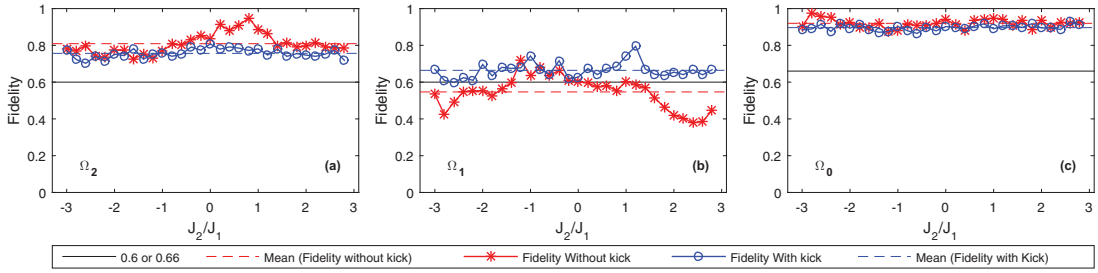


Fig. 4: (Colour online) (a) Fidelity of $\Omega_2$ state transfer with $E_1 = 0$ (red) and $E_1 = 1$ (blue). (b) Fidelity of $\Omega_1$ state transfer with $E_1 = 0$ (red) and $E_1 = 1$ (blue). (c) Fidelity of single-state transfer with $E_1 = 0$ (red) and $E_1 = 1$ (blue). All chains with parameter $J_2/J_1$ for $N = 10$, $J_1 = 1$ and $E_0 = 0.1$. The kicked electric field is seen to affect the fidelity.

Bell pair is transported. The fidelity is given by [25]

$$\bar{F}(t) = \frac{1}{3}\left(|f_{N-1,1}|^2 + |f_{N,2}|^2 + \frac{|f_{N-1,2}|^2}{2} + \frac{|f_{N,1}|^2}{2}\right) + \frac{1}{3}Re\left[f_{N,2}f^*_{N-1,1}\right] \quad (7)$$

for the Bell pair $|\Omega_1\rangle_{12} = b|01\rangle + c|10\rangle$, and

$$\bar{F}(t) = \frac{1}{2} - \frac{1}{6}\sum_{n=1}^{N-2}\left(|g^{n,N-1}_{1,2}|^2 + |g^{n,N}_{1,2}|^2\right) + \frac{1}{3}\left(|g^{N-1,N}_{1,2}|^2 + Re\left|g^{N-1,N}_{1,2}\right|\right) \quad (8)$$

for $|\Omega_2\rangle_{12} = a|00\rangle + d|11\rangle$ [25]. Here, $g^{b1,b2}_{a1,a2} = \langle b1, b2|\exp(-iHt)|a1, a2\rangle$. In this case, the subspace of the Hamiltonian corresponds to two spin-up excitations among all other spins in down polarized state.

**Results.** – Through studying the variation of fidelity transfer of a single state with the kick interval ($\tau$) for a pure chain with $E_1 = 1$, $J_1 = 1$, $J_2 = -1$ and $E_0 = 0.1$, we found that the fidelity has a periodic behaviour controllable by the kick interval ($\tau$). This emergence of periodicity helps us limit the number of kicks that are sufficient for obtaining the maximum fidelity for spin chains. The increment in number of kicks beyond a certain value is of no use as the fidelity pattern repeats. Now that we have an insight into the behaviour of fidelity with a control parameter, *i.e.*, time interval between the kicks, we move to ascertain the spin chain characteristics for efficient transmission of qubit(s) which is the central idea of the paper.

The chains have their maximum fidelity shown in all cases subject to variable kick interval $\tau$ (0.1 to 10) and also the number of kicks (up to 500). Without the kicked field, the chain is time evolved through the time interval ranging from 1 to 5000 in tune with the maximum time evolution considered for the kicked chain ($500 \times 10$). These parameters are controllable in a physical system and hence, may be tuned to achieve high fidelity as obtained in the simulation and the chain engineered to achieve the maximum fidelity (characterized by the $J_2/J_1$ ratio or impurity strength). For the first case, we compare the results of a spin chain with kicked electric field and without electric field as shown in fig. 4.

Typically, the fidelity of transfer for $\Omega_0$ remains low for such a system [9]. However, the electric field has a subtle positive effect on the fidelity of single-state transfer for some chains and also shows a normalizing behaviour as seen in fig. 4(c). It pushes up the otherwise low-in-fidelity chains (characterized by a value of $J_2/J_1$) and diminishes the difference of fidelity in different chains at the same time. However, some cases are found to have been negatively affected by electric-field kicks for single-state ($\Omega_0$) transfer.

Now we analyse the fidelity of transfer of two sets of Bell pairs in the same way as described above in fig. 4 (a), (b). It is observed that using the electric-field kicks improve the fidelity in case of $\Omega_1$ particularly. A large fidelity enhancement is obtained (reflected in the mean line position) and the normalizing behaviour is also seen. The state $\Omega_2$ is negatively affected by the kick subtly but shows the normalizing behaviour. However, the $\Omega_1$ state is poorly transferable in such a quantum channel with respect to a classical one albeit few peaks ($J_2/J_1 = -1$ to 0.8) are obtained beyond this limit even without the kicked electric field. It remains the worst amongst all states despite the enhancement in fidelity due to kicking. Chains characterized by $J_2/J_1 = -2$ to 3 (with some exceptions) are suitable for transfer of all the states as they are the only ones better than the classical ones (fig. 4(b)) or almost the same for transfer of $\Omega_1$ which exhibits least fidelity for transfer among all the states. We now select the ratio $J_2/J_1$ by seeing its performance in other input states. It is readily seen from fig. 4(a) that chains characterized by $J_2/J_1 = -1.6$ to 0.8 are the best for the $\Omega_2$ state as well. Now, turning to single-state transfer (fig. 4(c)), we see $J_2/J_1 = -1$ to be the best for our cause exhibiting a fidelity of $> 0.9$, although many other chains also suffice for our purpose. We are particularly interested in the case $J_2/J_1 = -1$ as a real material $LiCu_2O_2$ having approximately the same parameters can be tested experimentally. Now the electric field is changed for the selected chain as shown in fig. 5.

Except some deviations, it can be readily observed that as the kicked electric field is increased, the fidelity gener-

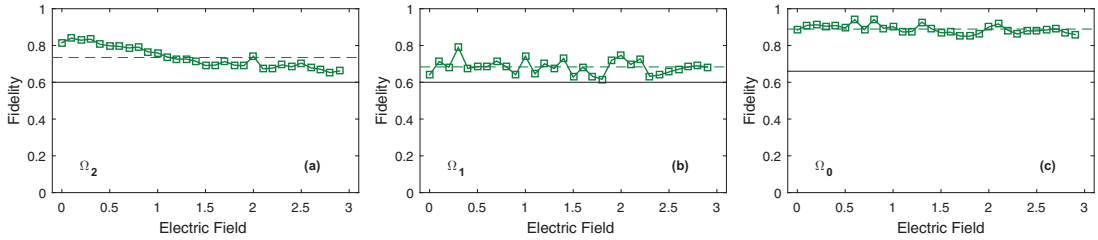


Fig. 5: (Colour online) (a) Fidelity of $\Omega_2$ state transfer. (b) Fidelity of $\Omega_1$ state transfer. (c) Fidelity of single-state transfer. All chains with parameter $E_1$ on the $x$-axis and $J_2/J_1 = -1$ for $N = 10$, $J_1 = 1$, $E_0 = 0.1$. The electric field is seen to affect fidelity.

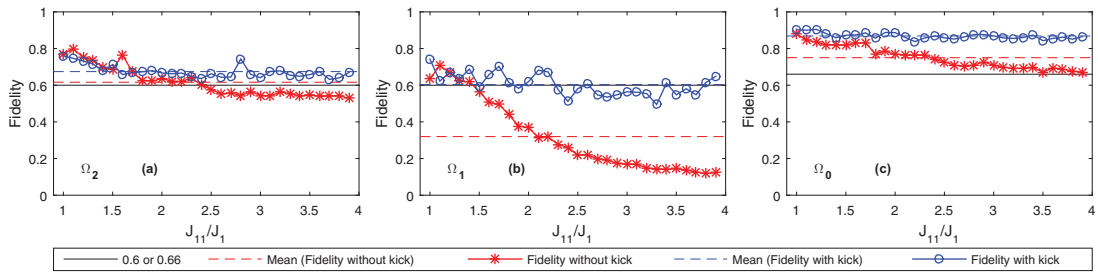


Fig. 6: (Colour online) (a) Fidelity of $\Omega_2$ state transfer with $E_1 = 0$ (red) and $E_1 = 1$ (blue). (b) Fidelity of $\Omega_1$ state transfer with $E_1 = 0$ (red) and $E_1 = 1$ (blue). (c) Fidelity of $\Omega_0$ state transfer with $E_1 = 0$ (red) and $E_1 = 1$ (blue). All chains taken with parameter larger nearest-neighbour exchange integral $J_{11}$ in chain as shown in fig. 2. The ratio $J_{11}/J_1$ which is indicative of bond size changes (increases), similarly $J_{22}/J_2$ (next-nearest-neighbour exchange ratio) and $J_{222}/J_2$ (next-nearest-neighbour exchange ratio) also change as shown in fig. 2. $N = 10$, $J_1 = 1$, $J_2 = -1$, $E_0 = 0.1$ and $E_1 = 1$. The kicked electric field is seen to affect fidelity.

ally decreases for $\Omega_2$ and increases for $\Omega_1$ whereas single-state transfer fidelity remains largely unaffected (fig. 5). Therefore, the optimum electric fields can be selected again by the peaks of $\Omega_1$ graph as it exhibits the minimum fidelity among all states considered. These are found to be 0.3, 1.0, 1.4. When considered for all the states $E_1 = 1$ is found to be the most suitable. Interestingly, in fig. 4, we considered $E_1 = 1$ which gives the optimum fidelity as found.

We now assess the impact of introduction of an impurity showing distinct compression between nearest and next-nearest spins (type I) with the exchange integral affected as discussed in the previous section. The variation of fidelity with increasing compression is shown in fig. 6. $J_{11}/J_1$ increases as the effect of impurity is increased and the compression also increases. Starting from $J_{11}/J_1 = J_{22}/J_2 = J_{222}/J_2 = 1$, the parameters are slowly changed to simulate increment in the compression and hence the strength of impurity. We have resorted to $LiCu_2O_2$ as the base material in which we embed the impurity and for which, $J_1 = 11 \pm 3\,\text{meV}$ and $J_2 = -7 \pm 1\,\text{meV}$ and hence, we can approximately assume $J_1 = 1$ and $J_2 = -1$ in appropriate energy scale. Correspondingly, the energy scale is in the ps regime, meaning that the electric-field pulses have to be in the sub-ps time scale for the impulsive approximation in eq. (5) to be valid.

There is a marked decrease in the fidelity of chains by the introduction of such an impurity and the increment in compression (strength) decreases the fidelity for all input states considered. For the case of two-qubit transfer, the already low fidelity for $\Omega_1$ is very low rendering it virtually useless for such a transfer especially in stronger impurity chains except for the one characterized by $J_{11}/J_1 = 1.2$ without kicking. But after kicking, some other chains characterized by $J_{11}/J_1 = 1.1, 1.2, 1.3, 1.4, 1.6, 1.7, 2.1$ and 2.2 are found suitable as seen from fig. 6(b). On comparing the fidelity for all states it is found that $J_{11}/J_1 = 1.7$ and 2.1 are the best choice.

The highest fidelity obtained for $\Omega_2$ was through the pure chain and was reduced by the kicking (although above 0.60). The electric field draws a kind of normalizing behaviour for all impurity strengths as is evident from fig. 6. In a way, it undermines the presence of impurity effectively for qubit(s) transfer though at an expense of higher fidelity $\Omega_2$ in some regime. This fidelity is lowered and normalized but the enhancement of fidelity for $\Omega_1$ works to our advantage. For single state also, it is seen to be advantageous (fig. 6(c)).

Hence, if we implement the kicking scheme with a chain characterized by a $J_{11}/J_1$ ratio of 1.7 or 2.1, we will be successfully transferring all the three states with sufficient fidelity (and relatively better than others). Now, we investigate the change in maximal fidelity for the selected chain characterized by such an impurity strength with the magnitude of the kicked electric field ($E_1$).

Here, an increase in fidelity is observed with increasing

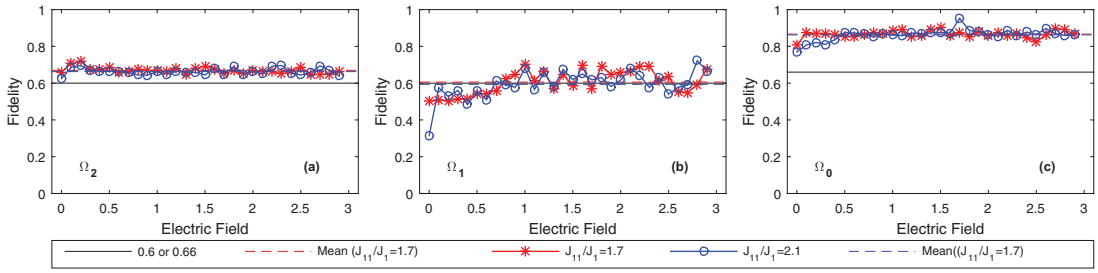


Fig. 7: (Colour online) (a) Fidelity of $\Omega_2$ state transfer. (b) Fidelity of $\Omega_1$ state transfer. (c) Fidelity of single-state transfer In all the cases the parameter is $E_1$ on the $x$-axis and $J_{11}/J_1 = 1.7$, $J_{22}/J_2 = 1.7$ and $J_{222}/J_2 = 0.825$ for the red graph and $J_{11}/J_1 = 2.1$, $J_{22}/J_2 = 2.1$ and $J_{222}/J_2 = 0.725$ for the blue graph. $N = 10$ , $J_1 = 1$ $J_2 = -1$ and $E_0 = 0.1$. The electric field is seen to affect fidelity.

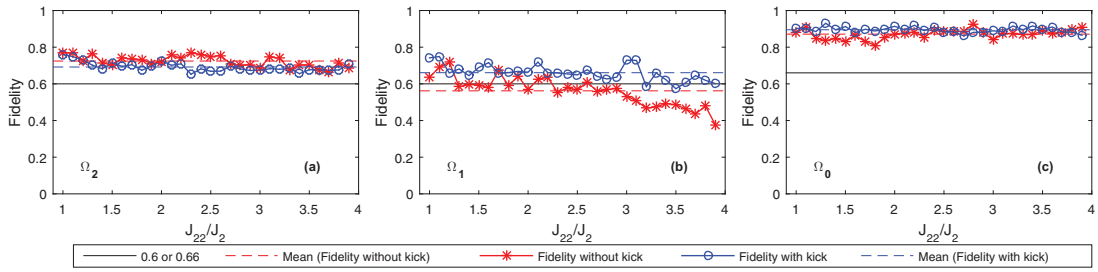


Fig. 8: (Colour online) (a) Fidelity of $\Omega_2$ state transfer with $E_1 = 0$ (red) and $E_1 = 1$ (blue). (b) Fidelity of $\Omega_1$ state transfer with $E_1 = 0$ (red) and $E_1 = 1$ (blue). (c) Fidelity of single-state transfer with $E_1 = 0$ (red) and $E_1 = 1$ (blue). All chains taken with shorter next-nearest-neighbour bond, *i.e.* larger next-nearest-neighbour exchange integral $J_{22}$ in chain as shown in fig. 2. The ratio $J_{22}/J_2$ which is indicative of bond size changes, similarly $J_{111}/J_1$ (next-nearest-neighbour exchange) and $J_{222}/J_2$ (longer next-nearest-neighbour exchange) also change as shown in fig. 2. $N = 10$, $J_1 = 1$, $J_2 = -1$ and $E_0 = 0.1$. The kicked electric field is seen to affect fidelity.

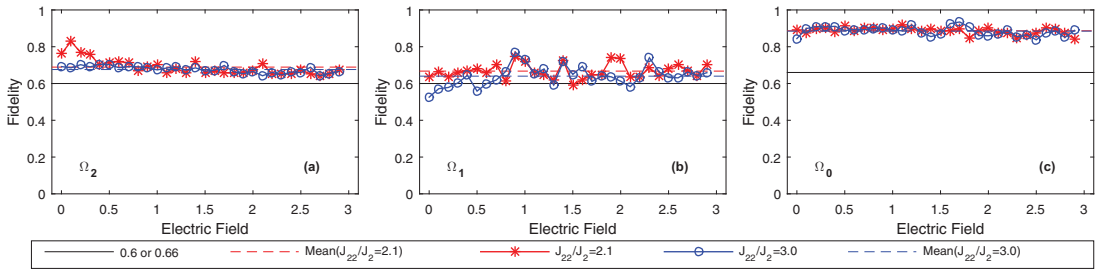


Fig. 9: (Colour online) (a) Fidelity of $\Omega_2$ state transfer. (b) Fidelity of $\Omega_1$ state transfer. (c) Fidelity of a single-state transfer. In all cases, the parameter is $E_1$ on the $x$-axis and $J_{22}/J_2 = 2.1$, $J_{222}/J_2 = 0.725$ and $J_{111}/J_1 = 0.725$ for the red graph and $J_{22}/J_2 = 3.0$, $J_{222}/J_2 = 0.50$ and $J_{111}/J_1 = 0.50$ for the blue graph. $N = 10$ , $J_1 = 1$ $J_2 = -1$ and $E_0 = 0.1$. The electric field is seen to affect fidelity.

the magnitude of the kicked electric field for single-state transfer (fig. 7(c)) and $\Omega_1$ (fig. 7(b)). However, the fidelity of transfer of $\Omega_2$ remains largely unaffected (fig. 7(a)). Also, the trends for both the spin chains are nearly the same. Again, $\Omega_1$ limits the choice of applied electric field through the kick to $E_1 = 1, 1.2, 1.4, 1.6$ and $E_1 = 1.8$ to 2.4 with some exceptions for both the chains. Isolated peaks at $E_1 = 2.8$ and $E_1 = 2.9$ are also observed.

We now calculate the fidelity in the presence of another type of impurity (type II) as discussed in the introduction section with resulting elongation between nearest and next-nearest spins. The exchange integrals are assumed to be affected in the same way as discussed in the introductory section. Starting from $J_{22}/J_2 = J_{222}/J_2 = J_{111}/J_1 = 1$, the parameters are slowly changed to simulate an increase in the impurity strength and the corresponding maximum fidelity is noted for all the input states considered. We again resort to $LiCu_2O_2$ as the base material for which we can approximately assume $J_1 = 1$ and $J_2 = -1$ in appropriate scale.

The results are the same as that obtained in last case of type-I impurities (fig. 6) with electric field again enhancing and normalizing the fidelity and subtle decrease in fidelity obtained for all input states as the impurity strength leading to local elongation is increased. Chains characterized by a $J_{22}/J_2 = 1.1, 1.2$ and 1.7 are found to

be the good as they allow transfer of $\Omega_1$ with sufficient fidelity even without kicking. By analysing fig. 8, we may well conclude that chains characterized by a $J_{22}/J_2$ ratio of 2.1, 3.0 and many others are suitable for transfer in all the three input cases with kicking. Now the selected chains characterized by a $J_{22}/J_2$ ratio of 2.1 and 3.0 are tested against varying electric field.

Once again a marked increase in fidelity is observed for $\Omega_1$ and $\Omega_0$. Fidelity for transfer of $\Omega_2$ shows subtle decrease with increase in electric field. The peaks in $\Omega_1$ as seen in fig. 9 restrict our choice of electric field to $E_1 \geq 0.8$ with some exceptions for different chains. We then move on to the transfer of $\Omega_2$ and $\Omega_0$ for the identification of a particular $E_1$ which is better suited for the complete job, which is again $E_1 \geq 0.8$, as not much advantage is offered by selecting a specific field.

**Conclusion.** – We have shown here the effectiveness of helical multiferroic chains in transferring both single qubit and Bell pairs ($\Omega_1$ and $\Omega_2$) from one end of the chain to the other end. Also, we have found some very interesting properties associated with the helical chains, *i.e* the periodicity of fidelity when subjected to pulsed (kicked) electric fields. By merely changing the kick interval, the periodicity is changed or even completely lost. We have also specifically identified the key parameters associated with efficient transfer of the qubits viz. electric field and impurity strength for two types of impurity. In the qubit(s) transfer protocol, the kick interval and number of kicks are also important for any particular chain to exhibit the desired fidelity. The recipe for a better transfer is straightforward and involves "kicking" the system (fig. 3) with electric fields at regular intervals (fig. 1). By carefully doping the actual material $LiCu_2O_2$ with the impurity whose effect on the exchange integral to the rest of the chain we have identified in various cases, the chain can be engineered to ensure high fidelity. At the same time, results also indicate that kicking the system by the electric field undermines the presence of impurity, and chains with distinct strengths of impurity show similar fidelity. This normalizing behaviour of the kicked electric field is seen in both types of impurity considered and for all the input states. Further, the role of the kicked electric field in transmission of qubits was ascertained by testing selected chains against the variation of the kicked electric field.

* * *

SKM acknowledges the Department of Science and Technology, India for support grant under the INSPIRE Faculty Fellowship award [IFA-12 PH 22].

REFERENCES

[1] Bose S., *Phys. Rev. Lett.*, **91** (2003) 207901.
[2] Amico L., Fazio R., Osterloh A. and Vedral V., *Rev. Mod. Phys.*, **80** (2008) 517.
[3] Arnesen M. C., Bose S. and Vedral V., *Phys. Rev. Lett.*, **87** (2001) 017901.
[4] Verstraete F., Murg V. and Cirac J. I., *Adv. Phys.*, **57** (2008) 143.
[5] Simon J., Bakr W. S., Ma R., Tai M. E., Preiss P. M. and Greiner M., *Nature*, **472** (2011) 307.
[6] Popp M., Verstraete F., Martín-Delgado M. A. and Cirac J. I., *Phys. Rev. A*, **71** (2005) 042306.
[7] De Chiara G., Lepori L., Lewenstein M. and Sanpera A., *Phys. Rev. Lett.*, **109** (2012) 237208.
[8] D'Arrigo A., Benenti G., Falci G. and Macchiavello C., *Phys. Rev. A*, **92** (2015) 062342.
[9] Azimi M., Chotorlishvili L., Mishra S. K., Greschner S., Vekua T. and Berakdar J., *Phys. Rev. B*, **89** (2014) 024424.
[10] Azimi M., Chotorlishvili L., Mishra S. K., Vekua T., übner W. H. and Berakdar J., *New J. Phys.*, **16** (2014) 063018.
[11] Chotorlishvili L., Azimi M., Stagraczynski S., Toklikishvili Z., Schüler M. and Berakdar J., *Phys. Rev. E*, **94** (2016) 032116.
[12] Azimi M., Sekania M., Mishra S. K., Chotorlishvili L., Toklikishvili Z. and Berakdar J., *Phys. Rev. B*, **94** (2016) 064423.
[13] Menzel M., Mokrousov Y., Wieser R., Bickel J. E., Vedmedenko E., Blugel S., Heinze S., Von Bergmann K., Kubetzka A. and Wiesendanger R., *Phys. Rev. Lett.*, **108** (2012) 197204.
[14] Masuda T., Zheludev A., Bush A., Markina M. and Vasiliev A., *Phys. Rev. Lett.*, **92** (2004) 039706.
[15] Schrettle F., Krohns S., Lunkenheimer P., Hemberger J., Büttgen N., Krug von Nidda H. A., Prokofiev A. V. and Loidl A., *Phys. Rev. B*, **77** (2008) 144101.
[16] Eerenstein W., Mathur N. D. and Scott J. F., *Nature*, **442** (2006) 759.
[17] Spaldin N. A. and Fiebig M., *Science*, **309** (2005) 391.
[18] Cheong S. W. and Mostovoy M., *Nat. Mater.*, **6** (2007) 13.
[19] Park S., Choi Y. J., Zhang C. L. and Cheong S. W., *Phys. Rev. Lett.*, **98** (2007) 057601.
[20] Bennett C. H., Brassard G., Crepeau C., Jozsa R., Peres A. and Wootters W. K., *Phys. Rev. Lett.*, **70** (1993) 1895.
[21] Moskalenko A. S., Zhu Z.-G. and Berakdar J., *Phys. Rep.*, **672** (2017) 1.
[22] Wang J., Guarneri I., Casati G. and Gong J., *Phys. Rev. Lett.*, **107** (2011) 234104; Poletti D. and Kollath C., *Phys. Rev. A*, **84** (2011) 013615; Wang H., Wang J., Guarneri I., Casati G. and Gong J., *Phys. Rev. E*, **88** (2013) 052919.
[23] Andrei N. and Johannesson H., *Phys. Lett. A*, **100** (1984) 108.
[24] Rogers R. N., Finegold L. and Morosin B., *Phys. Rev. B*, **6** (1972) 1058.
[25] Lorenzo S., Apollaro T. J. G., Paganelli S., Palma G. M. and Plastina F., *Phys. Rev. A*, **91** (2015) 042321.